Separation Science and Technology
Publication details, including instructions for authors and subscription information:
http://www.informaworld.com/smpp/title~content=t713708471

Prediction of Equilibria and Mass Transfer Rates in Continuous Foam Fractionation of Phosphate

Y. V. Nguyen[a]; C. R. Phillips[a]
[a] DEPARTMENT OF CHEMICAL ENGINEERING AND APPLIED CHEMISTRY, UNIVERSITY OF TORONTO, TORONTO, CANADA

To cite this Article Nguyen, Y. V. and Phillips, C. R.(1973) 'Prediction of Equilibria and Mass Transfer Rates in Continuous Foam Fractionation of Phosphate', Separation Science and Technology, 8: 1, 11 — 32

To link to this Article: DOI: 10.1080/00372367308057986

URL: http://dx.doi.org/10.1080/00372367308057986

SEPARATION SCIENCE, 8(1), pp. 11–32, 1973

Prediction of Equilibria and Mass Transfer Rates in Continuous Foam Fractionation of Phosphate

Y. V. NGUYEN and C. R. PHILLIPS

DEPARTMENT OF CHEMICAL ENGINEERING
AND APPLIED CHEMISTRY
UNIVERSITY OF TORONTO
TORONTO 181, CANADA

Abstract

An experimental investigation of the effect of the operating variables on the removal of phosphate in continuous foam fractionation using ethylhexadecyl dimethylammonium bromide as surfactant was performed. The removal of phosphate is described in terms of surface concentration of phosphage, and the operating variables are bubble residence time, concentration of phosphate, and pH of the bulk solution. Experimental equilibrium residence times agree well with those calculated from the Poisson equation of surface potential. The preferential adsorption ratio of divalent to monovalent phosphate is derived from the Gibbs equation, and is found to be six, based on a statistical correlation using the Langmuir adsorption isotherm.

INTRODUCTION

Foam fractionation is a method of removing and concentrating surface active solutes from a dilute solution. The process relies on the tendency of the surfactant molecules to accumulate at the gas–liquid interface. When solutes to be removed are not surface active, the addition of surfactant to the solution before foaming is necessary. Foam fractionation has been used successfully to remove the radioactive solutes, cesium, strontium, and cerium from a dilute solution (*1*, *2*). Microorganisms and inorganic colloids such as ferric oxide, stannic oxide, kaolin clay, and ferrocyanide complexes have also been separated by foam (*3–9*). Orthophosphate has been foam fractionated successfully with ethylhexadecyl dimethylammonium bromide (EHDA-Br) in batch operation (*10–12*) and in continuous operation (*13*). The intention of this work is to provide information on the mechanism of phosphate removal and on the equilibrium between the surface and the bulk phases for phosphate of different ionic forms.

THEORY

The Mass Transfer Equations

The mechanism of phosphate removal in foam fractionation involves either the formation of surfactant phosphate complex, which diffuses to the surface of gas–liquid interface, and/or the adsorption of surfactant followed by the electrostatic attraction between surfactant and the oppositely charged phosphate. Regardless of which mechanism the transfer process follows, there must be a finite time for phosphate to reach the equilibrium surface concentration. Equilibrium is established when the rate of adsorption equals the rate of desorption (*14*):

$$\left(\frac{d\Gamma}{dt}\right)_{\text{ads}} = B_1 x(1 - \theta) \tag{1}$$

$$-\left(\frac{d\Gamma}{dt}\right)_{\text{des}} = B_2 \Gamma \exp\left\{\frac{ze\psi_0 - W}{kT}\right\} \tag{2}$$

where B_1 and B_2 are constants depending on the hydrodynamics of the diffusion process, ψ_0 is the surface potential, W is the energy of desorption of the hydrocarbon chain, z is the valency of the long-chain ion, e is electronic charge, k is the Boltzmann constant, T is the absolute temperature, θ is the fraction of surface already covered with molecules, and Γ is the concentration of surfactant phosphate complex on the surface.

The energy of desorption can be evaluated by an empirical expression (*14*):

$$\frac{W}{kT} = \frac{521m}{RT} + \frac{1200 \times 10^{-8} m(\Gamma N_{\text{av}})^{1/2}}{k'T} \tag{3}$$

where m is the effective number of —CH$_2$— groups of the long hydrocarbon chain, $k' = k \times 10^{16}$, and N_{av} is the Avogadro number.

If θ is small and if W and ψ_0 are sensibly constant, the net rate equation would be

$$\left(\frac{d\Gamma}{dt}\right)_{\text{net}} = B_2 \exp\left\{\frac{ze\psi_0 - W}{kT}\right\}(\Gamma_e - \Gamma) \tag{4}$$

where subscript e denotes the equilibrium condition.

For the present work, the net rate of adsorption could be written in terms of a surface mass transfer coefficient h:

$$\left(\frac{d\Gamma}{dt}\right)_{\text{net}} = h(\Gamma_e - \Gamma) \tag{5}$$

where h can be evaluated by graphical integration of the surface concentration of phosphate:

$$h = \Gamma_e \Big/ \int_0^\infty (\Gamma_e - \Gamma)\, dt \tag{6}$$

The equilibrium residence time can be evaluated by integration of Eqs. (4) and (5):

$$\left(\frac{\Gamma}{\Gamma_e}\right)_B = \frac{\exp\left(tB_2 \exp\{ze\psi_0 - W/kT\}\right) - 1}{\exp\left(tB_2 \exp\{ze\psi_0 - W/kT\}\right)} \tag{7}$$

or

$$\left(\frac{\Gamma}{\Gamma_e}\right)_h = \frac{e^{ht} - 1}{e^{ht}} \tag{8}$$

For the system of EHDA-Br and phosphate, the surface potential ψ_0 is the solution of the Poisson equation

$$\nabla^2\psi = \frac{8\Pi\rho e}{D}\, x_{\text{EHDA}} + \sinh\left\{\frac{e\psi}{kT}\right\} - \frac{8\Pi\rho e}{D}\, x_{\text{HPO}_4^{-2}} \times \left(\exp\left\{\frac{e\psi}{kT}\right\} - \exp\left\{\frac{2e\psi}{kT}\right\}\right) \tag{9}$$

This equation was obtained from the Boltzmann distribution of charge and a charge balance in the solution (*15*).

In the absence of divalent phosphate and at room temperature, the surface potential ψ_0 can be obtained (*14*, *15*)

$$\psi_0 = 51.5 \sinh^{-1}\left\{\frac{135}{A x_{\mathrm{EHDA}^+}^{1/2}}\right\} \tag{10}$$

where ψ_0 is in millivolts, A is the area available for the EHDA$^+$ ion on the surface (in Å^2), and x_{EHDA^+} is the concentration of EHDA$^+$ (g mole/l) in the solution.

Preferential Adsorption

The thermodynamic relationship between the surface excess of the components of the solution and the surface tension and chemical potentials of all components in the solution has been derived by Gibbs (*14*, *16*):

$$(d\gamma)_T = -\Sigma\Gamma\, d\mu \tag{11}$$

The Gibbs equation can be used to explain the preferential adsorption of divalent phosphate to monovalent phosphate at constant surfactant concentration.

Consider a solution of monovalent phosphate and EHDA-Br. The system would involve the following equilibria:

$$\mathrm{EHDA\text{-}Br} \rightarrow \mathrm{EHDA}^+ + \mathrm{Br}^-$$

$$\mathrm{EHDA\text{-}H_2PO_4} \rightleftharpoons \mathrm{EHDA}^+ + \mathrm{H_2PO_4}^-$$

with the equilibrium constant K_1 defined for the second equilibrium

$$K_1 = \frac{[\mathrm{EHDA}^+][\mathrm{H_2PO_4}^-]}{[\mathrm{EHDA\text{-}H_2PO_4}]}$$

Application of the Gibbs equation together with the surface neutrality condition $\Gamma_{\mathrm{EHDA}^+} = \Gamma_{\mathrm{Br}^-} + \Gamma_{\mathrm{H_2PO_4}^-}$ results in the following relationship:

$$-(\Gamma_{\mathrm{H_2PO_4}^-} + \Gamma_{\mathrm{EHDA-H_2PO_4}}) = \frac{d\gamma + RT\Gamma_{\mathrm{Br}} - d\ln([\mathrm{EHDA}^+][\mathrm{Br}^-])}{RT\, d\ln([\mathrm{H_2PO_4}^-][\mathrm{EHDA}^+])} \tag{12}$$

At constant surfactant concentration, Eq. (12) becomes

$$-(\Gamma_{\mathrm{H_2PO_4^-}} + \Gamma_{\mathrm{EHDA-H_2PO_4}}) = \frac{x_{\mathrm{EHDA-H_2PO_4}}}{RT}\left(\frac{d\gamma}{dx_{\mathrm{EHDA-H_2PO_4}}}\right)_{\mathrm{EHDA-Br}} - \frac{\Gamma_{\mathrm{Br^-}}x_{\mathrm{H_2PO_4^-}}}{K_1} \tag{13}$$

For a solution of divalent phosphate and EHDA-Br, the Gibbs equation at constant surfactant concentration would become

$$-(\Gamma_{\mathrm{HPO_4^{-2}}} + \Gamma_{\mathrm{EHDA_2-HPO_4}}) = \frac{x_{\mathrm{EHDA_2-HPO_4}}}{RT}\left(\frac{d\gamma}{dx_{\mathrm{EHDA_2-HPO_4}}}\right)_{\mathrm{EHDA-Br}} - \frac{2\Gamma_{\mathrm{Br^-}}x_{\mathrm{HPO_4^{-2}}}(x_{\mathrm{Br^-}} - 2x_{\mathrm{EHDA_2-HPO_4}})}{K_2} \tag{14}$$

with K_2 defined as

$$K_2 = \frac{[\mathrm{EHDA^+}]^2[\mathrm{HPO_4^{-2}}]}{[\mathrm{EHDA_2\text{-}HPO_4}]}$$

The preferential adsorption of divalent phosphate to monovalent phosphate would be the ratio of Eqs. (14) and (13) when the total bulk concentration of phosphate and its complex in the solution are equal, i.e., when

$$x_{\mathrm{H_2PO_4^-}} + x_{\mathrm{EHDA-H_2PO_4}} = x_{\mathrm{HPO_4^{-2}}} + x_{\mathrm{EHDA_2-HPO_4}} \tag{15}$$

$$\frac{(\Gamma_{\mathrm{HPO_4^{-2}}} + \Gamma_{\mathrm{EHDA_2-HPO_4}})}{(\Gamma_{\mathrm{H_2PO_4^-}} + \Gamma_{\mathrm{EHDA-H_2PO_4}})} = \frac{2\Gamma_{\mathrm{Br^-}}x_{\mathrm{HPO_4^{-2}}}(x_{\mathrm{Br^-}} - 2x_{\mathrm{EHDA_2-HPO_4}})/K_2 - (d\gamma/dx_{\mathrm{EHDA_2-HPO_4}})_{\mathrm{EHDA-Br}}x_{\mathrm{EHDA_2-HPO_4}}/RT}{\Gamma_{\mathrm{Br^-}}x_{\mathrm{H_2PO_4^-}}/K_1 - (d\gamma/dx_{\mathrm{EHDA-H_2PO_4}})_{\mathrm{EHDA-Br}}x_{\mathrm{EHDA-H_2PO_4}}/RT} \tag{16}$$

The preferential adsorption could also be obtained by using the Langmuir adsorption isotherm for dilute solutions:

$$\Gamma_e = Kx \tag{17}$$

This type of equation is the result of Eqs. (1) and (2) when the rate of adsorption equals the rate of desorption (*14*):

$$\Gamma_e = \frac{(B_1/B_2)\exp([W - ze\psi_0]/kT)x}{1 + x(B_1/\Gamma_0 B_2)\exp([W - ze\psi_0]/kT)} \tag{18}$$

For dilute solution, Eq. (18) has the form of Eq. (17)

$$\Gamma_e = \frac{B_1}{B_2} \exp\left\{\frac{W - ze\psi_0}{kT}\right\} x \tag{19}$$

with

$$K = \frac{B_1}{B_2} \exp\left\{\frac{W - ze\psi_0}{kT}\right\} \tag{20}$$

The Langmuir equation can be applied to the system of phosphate and EHDA-Br

$$\Gamma_e = \beta_1 x_{\mathrm{H_2PO_4}^-} + \beta_2 x_{\mathrm{HPO_4}^{-2}} + \beta_3 x_{\mathrm{PO_4}^{-3}} \tag{21}$$

The ratio of β_2/β_1 is equivalent to

$$\frac{(\Gamma_{\mathrm{HPO_4}^{-2}} + \Gamma_{\mathrm{EHDA_2-HPO_4}})}{(\Gamma_{\mathrm{H_2PO_4}^-} + \Gamma_{\mathrm{EHDA-H_2PO_4}})}$$

of Eq. (16), and this ratio could be used as a preferential adsorption ratio of divalent to monovalent phosphate.

EXPERIMENTAL

The apparatus is shown schematically in Fig. 1. The feed solution was prepared by dissolving EHDA-Br and KH_2PO_4 in distilled water. The pH of the solution was adjusted by KOH and a minute quantity of HCl when necessary. The cylindrical foaming column was made of Pyrex and was 4.7 cm inside diameter and 105 cm in height. The bottom of the foam column consisted of a rubber stopper which could be moved up and down the column. The location of the feed inlet and the movability of the bottom of the foam column facilitated studies of phosphate removal at different depths of liquid. Foam was collapsed in a mechanical foam breaker consisting of a 12-slot basket rotated by a motor. The inside of the basket was covered with an 80-mesh stainless steel screen. Photographs of bubbles were taken and were analyzed on an electronic graph digitizer which gave a magnification ratio between 17 and 23 times.

Collected data in terms of gas, liquid flow rates, phosphate concentrations, bubble diameters, liquid column depths, and gas void fractions were converted to phosphate surface concentration and bubble residence times for analysis.

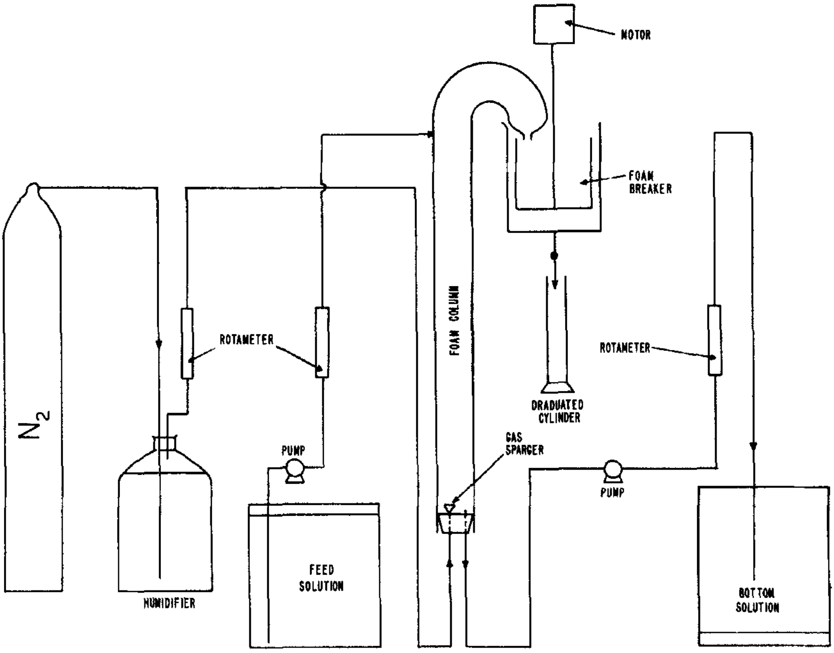

Fig. 1. Schematic representation of the equipment.

DISCUSSION

The effect of surfactant concentration on the removal of phosphate has been studied elsewhere (*13*). Here, unless otherwise specified, experiments were performed at 200 ppm EHDA-Br concentration. This is well below the critical micelle concentration (*13*).

Saturated Adsorption

Since the mechanism of phosphate removal involves either the diffusion of the surfactant phosphate complex to the gas–liquid interface and/or the adsorption of $EHDA^+$ followed by electrostatic attraction between $EHDA^+$ and phosphate, the bubble residence time is the prime factor in determining equilibrium for surface adsorption. The residence time is affected by the length of the liquid pool and by the gas flow rate. Figures 2 and 3 show the effect of liquid column length on the surface concentra-

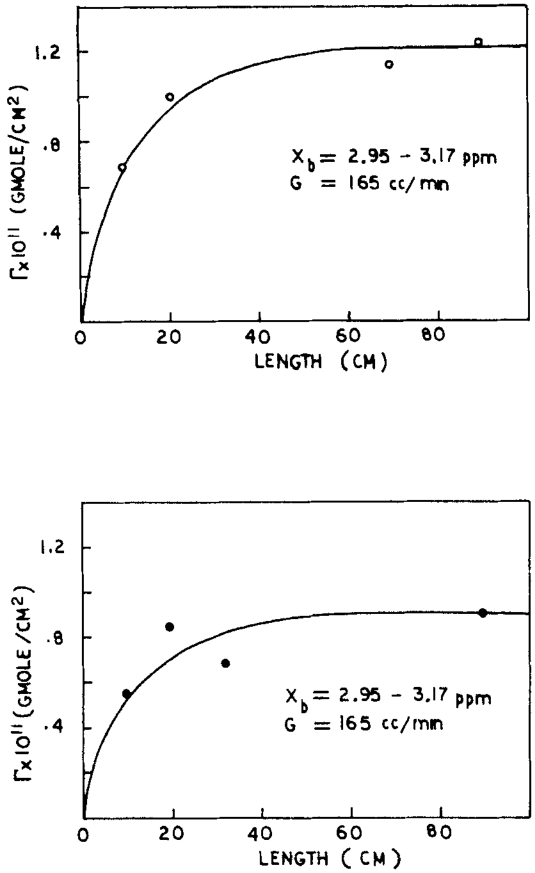

FIG. 2. Phosphate surface concentration as a function of liquid column length at pH 9.6 (top) and pH 7.0 (bottom).

tion of phosphate at phosphate bulk concentrations of 3 and 9 ppm. For a lower bulk concentration of phosphate, the rate of arrival of molecules at the surface is low, and therefore a longer column length is expected before equilibrium surface concentration can be established. This can be seen in Fig. 2.

The effect of gas rate on the surface concentration of phosphate is obscured by the effect of interstitial liquid between the foam bubbles. As the gas rate is increased, more interstitial liquid is carried between the foam bubbles, and this increases the collapsed foam flow rate which in turn reduces the phosphate collapsed foam concentration (*13*). The counter effect is the increase in surface area as the gas rate increases. This allows more phosphate to be removed if bubbles stay in the liquid column long enough for surface equilibrium to be achieved. In general the second effect overcomes the first one (see Fig. 4) if sufficient residence time is allowed. Figure 4 shows that there is a lower phosphate concentration in the outlet stream at a gas rate of 390 cm³/min than at a gas rate of 98 cm³/min. The effects of the length of the liquid pool and the gas flow rate on the surface concentration of phosphate can be combined into one single effect, residence time:

$$t = l/U_B$$

where l is the length of liquid pool and U_B is the bubble average velocity calculated from Nicklin's equation (*17*).

Figures 5 and 6 show the effect of residence time on the surface concentration of phosphate. The lower value of equilibrium residence time at high bulk phosphate concentrations is most probably due to the higher concentration driving force which results in a higher rate of mass trans-

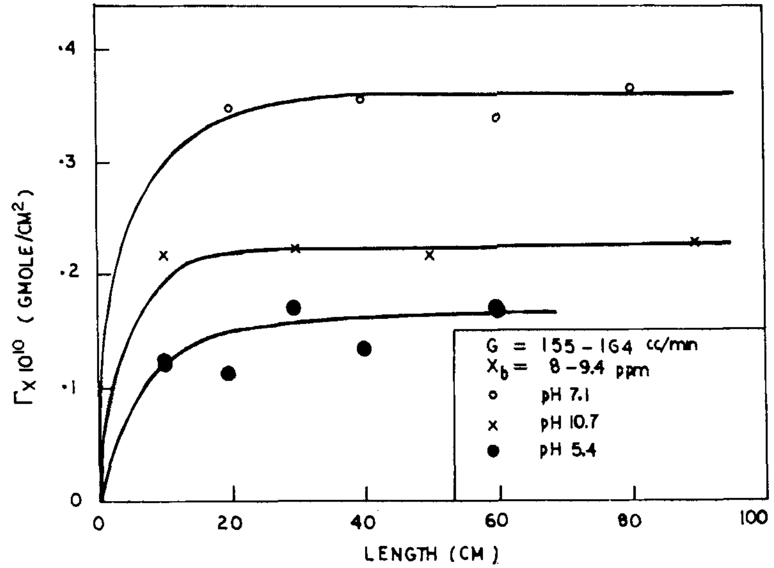

FIG. 3. Phosphate surface concentration as a function of liquid column length at different pH.

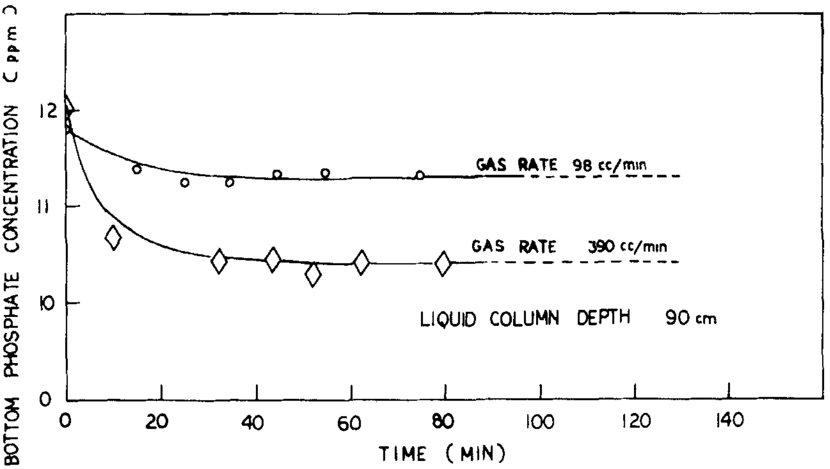

FIG. 4. Effect of time on bottom phosphate concentration.

fer of phosphate to the surface. If it were assumed that the removal of phosphate, besides the adsorption of surfactant phosphate complex, were due to the electrostatic attraction of phosphate by the presence of EHDA$^+$ on the surface, the surface potential ψ_0 of a solution of 200 ppm EHDA-Br and phosphate could be approximated by Eq. (10). With

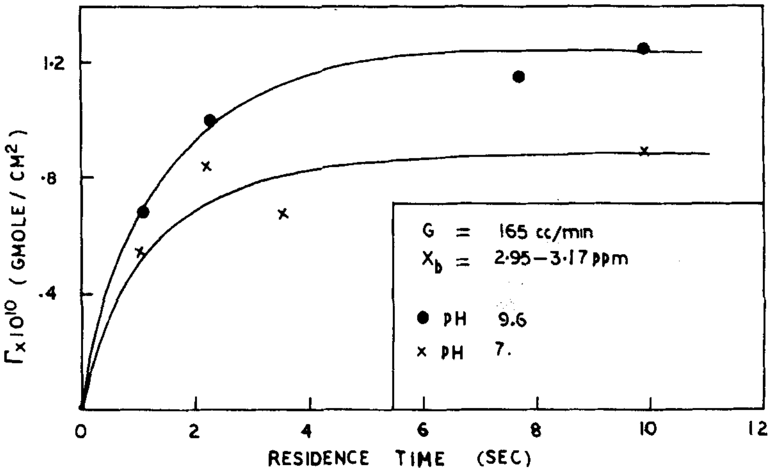

FIG. 5. Phosphate surface concentration as a function of residence time.

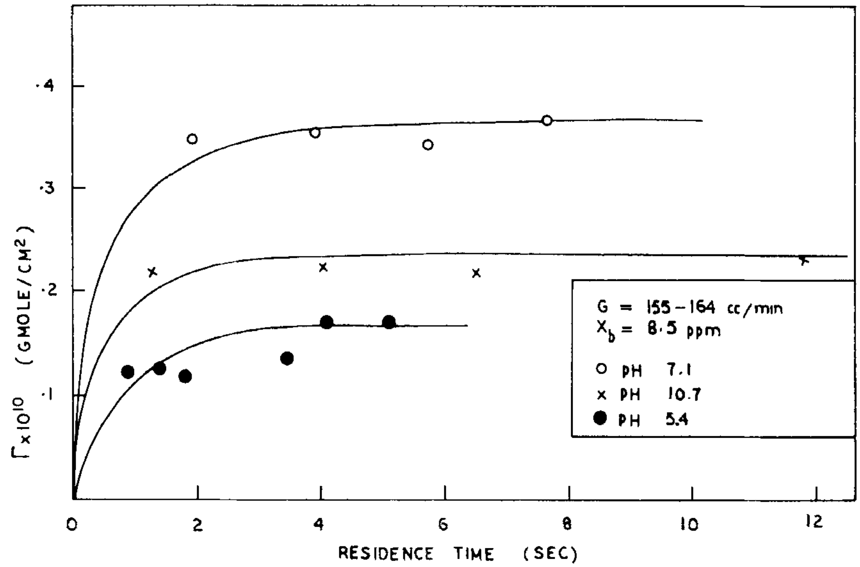

FIG. 6. Phosphate surface concentration as a function of residence time at different pH levels.

surface concentration of $EHDA^+$ of the order of 10^{-10} g mole/cm² (*13*), the surface potential ψ_0 calculated from Eq. (10) has a value of 222 mV. The net rate of phosphate transferred to the surface was evaluated by using Eq. (4) with the value of 2×10^4 sec^{-1} for B_2 obtained for cetyltrimethylammonium bromide (*14*). Comparison between Eqs. (4) and (5) show that $B_2 \exp([ze\psi_0 - W]/kT)$ of Eq. (4) is identical to the surface mass transfer coefficient h of Eq. (5). This surface mass transfer coefficient was evaluated by graphical integration of Γ values (Eq. 6). The good agreement between coefficients $B_2 \exp([ze\psi_0 - W]/kT)$ and h as seen from Table 1, especially when the predominant form of phosphate is $H_2PO_4^-$ (i.e., pH 5.4), confirms that the adsorption of phosphate was due to the presence of $EHDA^+$ on the surface. The slight differences between these coefficients at other pH conditions were due to the presence of divalent phosphate which was not taken into account in Eq. (10). With the mechanism of adsorption described above, the equilibrium residence time can be approximated by Eqs. (7) and (8) (see Fig. 7). Since the exact value of ψ_0 when divalent phosphate is present in the solution was not known, a statistical correlation was used to obtain the

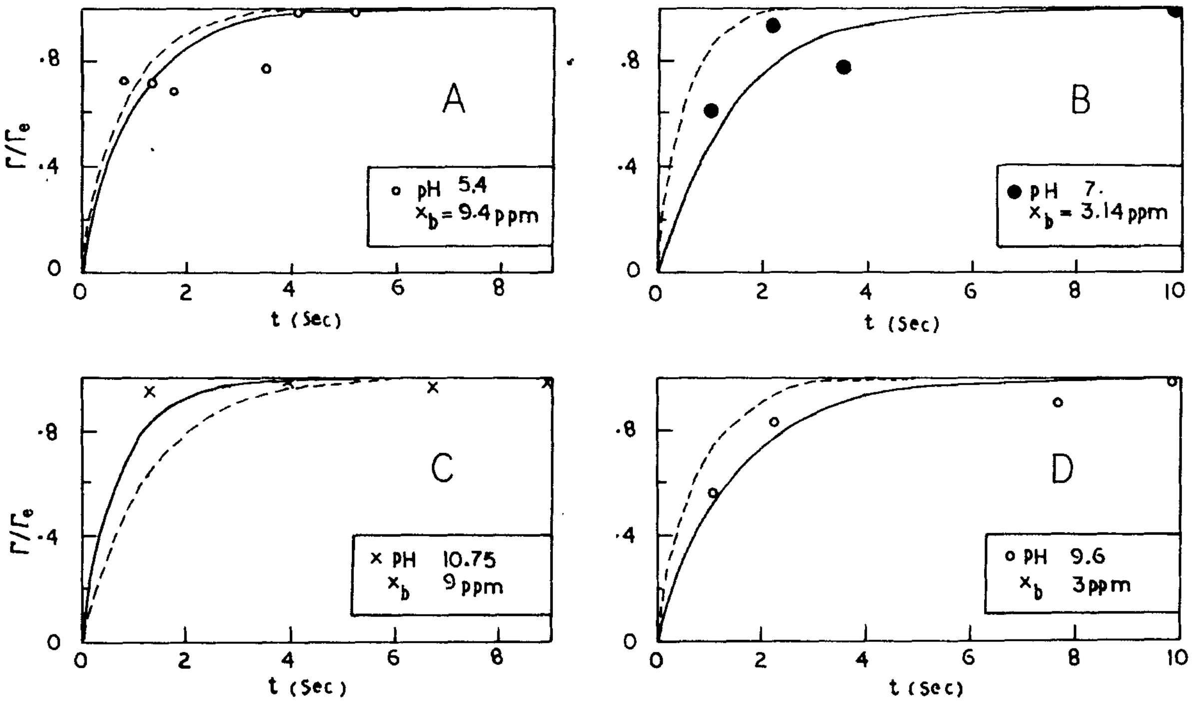

FIG. 7. Fraction of Γ/Γ_e as a function of residence time at different phosphate bulk concentrations. (——) Equation (8). (- -) Equation (7).

TABLE 1

Comparison between Experimental and Calculated Results

Residence time (sec)	Bulk concentration of phosphate (ppm)	Surface concentration of phosphate (g mole/cm^2)	pH of the bulk solution	Calculated surface mass transfer coefficient h (sec^{-1})	Calculated coefficient $B_2 \exp\left\{\frac{-W}{kT} + \frac{e\psi_0}{kT}\right\}$ (sec^{-1})
1.31	9.24	2.18×10^{-11}	10.75	1.31	0.82
4.0	9.89	2.22×10^{-11}	10.70	1.31	0.80
6.6	8.98	2.17×10^{-11}	10.75	1.31	0.81
11.8	8.95	2.27×10^{-11}	10.70	1.31	0.78
2.0	7.99	3.51×10^{-11}	7.07	1.25	0.47
3.9	8.21	3.58×10^{-11}	7.07	1.25	0.46
5.7	8.30	3.39×10^{-11}	7.10	1.25	0.62
7.7	8.30	3.68×10^{-11}	7.10	1.25	0.47
0.9	9.30	1.24×10^{-11}	5.4	1.01	1.29
1.4	9.38	1.22×10^{-11}	5.5	1.01	1.33
1.8	9.31	1.17×10^{-11}	5.55	1.01	1.37
4.1	9.46	1.71×10^{-11}	5.5	1.01	1.01
3.5	8.84	1.34×10^{-11}	5.8	1.01	1.16
5.1	8.77	1.71×10^{-11}	5.65	1.01	1.01
1.1	3.13	0.54×10^{-11}	$\simeq 7$	0.74	2.26
2.2	3.13	0.84×10^{-11}	$\simeq 7$	0.74	1.65
3.5	3.14	0.68×10^{-11}	$\simeq 7$	0.74	1.94
9.9	3.17	0.89×10^{-11}	$\simeq 7$	0.74	1.60
1.1	3.20	0.70×10^{-11}	$\simeq 9.6$	0.69	1.82
2.3	3.11	1.05×10^{-11}	$\simeq 9.6$	0.69	1.43
7.7	2.98	1.14×10^{-11}	$\simeq 9.6$	0.69	1.49
9.9	3.06	1.25×10^{-11}	$\simeq 9.6$	0.69	1.30

average equilibrium residence time at different operating conditions. On the basis of Eqs. (7) and (8), the statistical model takes the form

$$\frac{\Gamma}{\Gamma_e} = \frac{\exp(\alpha t) - 1}{\exp(\alpha t)} \tag{22}$$

from which $\alpha = 0.817$ sec^{-1}, evaluated by the Newton-Raphson method. The standard error is 8.5%. From Fig. 8 and Eq. (22), over 99% of the surface saturation can be obtained at residence times of less than 7 sec.

For all other experimental runs, gas rates and liquid column lengths

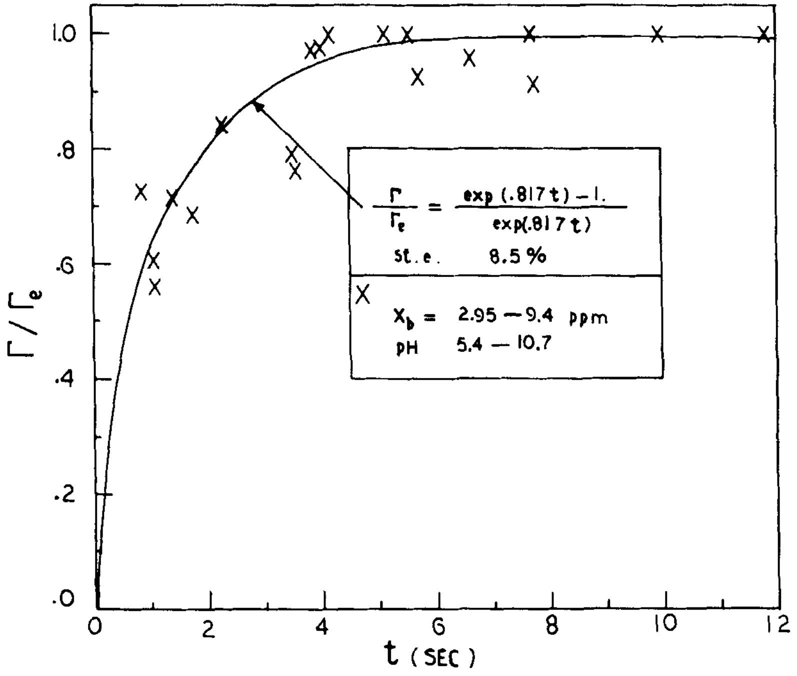

FIG. 8. Ratio of Γ/Γ_e as a function of residence time.

were so adjusted that the bubble residence time always exceeded 7 sec to ensure surface saturation of phosphate.

Preferential Adsorption

pH has a marked effect on the removal of phosphate (see Fig. 9). A change in pH would result in a change in concentration of the ionic forms of phosphate. At pH 5 more than 99% of phosphate is present in the form $H_2PO_4^-$, and at pH 8 the predominant form of phosphate is HPO_4^{-2}. In batch operation it is difficult to draw conclusions about the effect of pH on the removal of phosphate because the pH changes as experiments progress. The concentration of phosphate in the bulk solution also has a marked effect on the surface concentration of phosphate in continuous operation (see Fig. 10). As can be seen from Fig. 10, the surface concentration of phosphate increases with the bulk phosphate concentration. The scatter is probably due to the presence of different ionic forms of phosphate within the range of pH investigated.

Preferential adsorption of divalent to monovalent phosphate could be obtained by using experiments over a wide range of pH (pH 3 to 10.7) and phosphate bulk concentration (3.6 to 80 ppm of phosphate expressed as PO_4). The concentrations of the three ionic forms of phosphate were calculated from the three stepwise ionizations of phosphoric acid and from the measured pH of the bulk solution. Since the presence of EHDA-Br did not significantly alter the pH of the bulk solution, e.g., pH was 5 and 5.05 before and after addition of EHDA-Br, and since there might exist the surfactant phosphate complexes EHDA-H_2PO_4, $EHDA_2$-HPO_4, $EHDA_3$-PO_4, the concentration of the three ionic forms calculated above should be regarded as an approximation to the sum of the ionic and complex form of phosphate.

Within the range of pH used, phosphate was present in three forms, and a multidimensional plot with $[H_2PO_4^-]$, $[HPO_4^{-2}]$ and $[PO_4^{-3}]$ as coordinates could represent the surface equilibrium. This is unfortunately awkward in practice. Instead a stepwise regression analysis was used to describe the effect of the different ionic forms of phosphate on the total surface concentration.

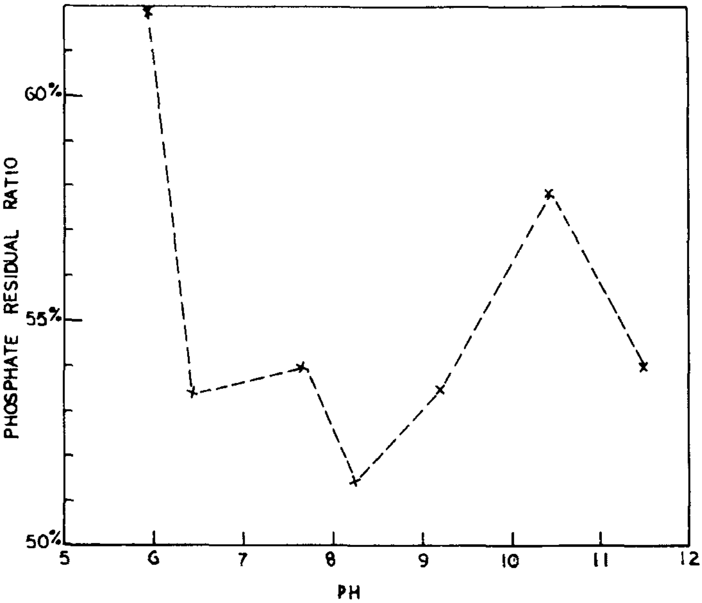

FIG. 9. Effect of pH on the removal of phosphate in batch operation.

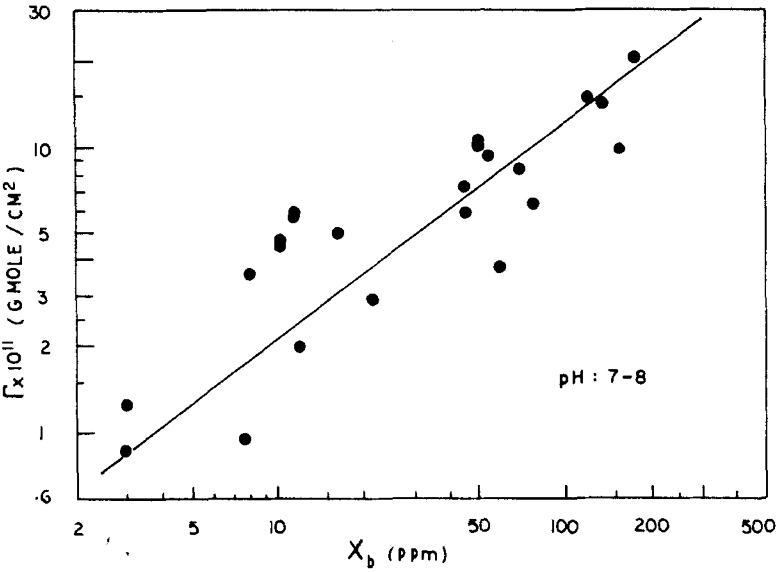

FIG. 10. Logarithmic plot of phosphate surface concentration vs. its bulk concentration.

Twenty-three regression models were used to describe these phenomena. The general form of the regression was

$$\Gamma_e = \beta_1 X_1 + \beta_2 X_2 + \beta_2 X_3 + \beta_{11} X_1^2 + \beta_{22} X_2^2 + \beta_{33} X_3^2 + \beta_{12} X_1 X_2 + \beta_{13} X_1 X_3 + \beta_{23} X_2 X_3 + \beta_0$$

where Γ_e is the total surface concentration of phosphate (in g mole/cm^2), β's are the linear regression coefficients,

$$X_1 = x_{\mathrm{H_2PO_4^-}} + x_{\mathrm{EHDA-H_2PO_4}}$$

$$X_2 = x_{\mathrm{HPO_4^{-2}}} + x_{\mathrm{EHDA_2-HPO_4}}$$

$$X_3 = x_{\mathrm{PO_4^{-3}}} + x_{\mathrm{EHDA_3-PO_4}}$$

and X_1, X_2, and X_3 are expressed in ppm of PO_4 to facilitate the calculation in a linear least square regression.

Since repeatability is fairly poor, the pure error analysis of variance was not used to analyze the data. Instead, the multiple correlation coefficient was used as a criterion of data fitting.

A backward elimination method was used to reduce the number of parameters in the model. A final linear model with rejection of four unusually bad data points is shown in Table 2. From Table 2 the regressed linear model has the form

$$\Gamma_e = \beta_1X_1 + \beta_2X_2 + \beta_3X_3 + \beta_{12}X_1X_2 + \beta_0 \tag{23}$$

with

$$\beta_1 = 0.148 \times 10^{-12}$$
$$\beta_2 = 1.221 \times 10^{-12}$$
$$\beta_3 = -0.1386 \times 10^{-10}$$
$$\beta_{12} = 0.1504 \times 10^{-12}$$
$$\beta_0 = 0.194 \times 10^{-10}$$

TABLE 2

Regressed Model

$$\Gamma_e = \beta_1X_1 + \beta_2X_2 + \beta_3X_3 + \beta_{12}X_1X_2 + \beta_0$$

The Coefficients and Their Standard Deviations and the *T*-values

Coefficients	Standard deviations	Student *T*
0.14813×10^{-12}	0.98085×10^{-13}	0.15102×10^{1}
0.12214×10^{-11}	0.13140×10^{-12}	0.92956×10^{1}
-0.13856×10^{-10}	0.58223×10^{-11}	-0.23797×10^{1}
0.15035×10^{-12}	0.39518×10^{-13}	0.38045×10^{1}

The constant is 0.19382×10^{-10}

Multiple correlation coefficient: 91.38609%

Analysis of Variance for the Model

Source	Degree of freedom	Sum of squares	Mean squares	Overall *F*
Regression	4	$0.10614969 \times 10^{-19}$	$0.2653742 \times 10^{-20}$	0.47741103×10^{2}
Residual	18	$0.10005499 \times 10^{-20}$	$0.5558611 \times 10^{-22}$	
Total	22	$0.116155.8 \times 10^{-19}$	$0.5279781 \times 10^{-21}$	

The constant parameter β_0 was included in the model to give a good fit without the necessity of using a high parameter model. Since β_0 was included, it is recommended that the model not be used to predict equilibrium phosphate surface concentration below 1.94×10^{-11} g mole/cm^2, which is approximately equivalent to 3 ppm of phosphate in the bulk solution.

Although the statistical model does not describe the actual mechanism of adsorption, the values of the β's can be used to determine the effect of different phosphate species.

The large negative value of parameter β_3 explains the reduction of total phosphate surface concentration when PO_4^{-3} and its complex are present in the bulk solution of mono- and divalent phosphate. The negativity of coefficient β_3 does not imply that a negative surface concentration would be obtained if the trivalent phosphate was the only form of phosphate in the bulk solution because PO_4^{-3} is present alone when the pH is higher than 14, a situation not encountered in this work.

Comparison of coefficients β_1 and β_2 shows that divalent phosphate is more preferentially adsorbed than monovalent phosphate. The adsorption ratio of divalent to monovalent phosphate β_2/β_1 is approximately six. This result is consistent with other investigator's work in the field of preferential adsorption (*2*). Wace (*2*) investigated the adsorption of divalent strontium and monovalent cesium and the results showed that strontium is more readily adsorbed than cesium. The preferential adsorption is most probably a consequence of employing a two-dimensional foaming system.

Besides the adsorption of the ions $H_2PO_4^-$, HPO_4^{-3}, and PO_4^{-3}, the removal of phosphate is due to the adsorption of the soluble surfactant-phosphate complexes [EHDA-H_2PO_4, $(EHDA)_2$-HPO_4, $(EHDA)_3$-PO_4]. Thus the complexed molecule having more EHDA$^+$ groups should be more readily adsorbed at the surface because of its lower affinity for the solvent molecules. It would be expected that $(EHDA)_3$-PO_4 would give the best separation; however, there is a higher steric hindrance effect for locating the molecules $(EHDA)_3$-PO_4 on a two-dimensional foaming system. Thus $(EHDA)_2$-HPO_4 is the most appropriate type of surfactant phosphate complex for the best separation of phosphate.

To further explain the effect of pH on the surface concentration of phosphate complexes, two independent solutions of the same initial concentration C_0 of EHDA-H_2PO_4 and $(EHDA)_2$-HPO_4 are considered.

$$\text{EHDA-}H_2PO_4 = \text{EHDA}^+ + H_2PO_4^-$$

$$(\text{EHDA})_2\text{-}HPO_4 = 2\text{EHDA}^+ + HPO_4^{-2}$$

with equilibrium constants defined as

$$K_1 = \frac{[\mathrm{EHDA}^+][\mathrm{H_2PO_4}^-]}{[\mathrm{EHDA\text{-}H_2PO_4}]}$$

and

$$K_2 = \frac{[\mathrm{EHDA}^+]^2[\mathrm{HPO_4}^{-2}]}{[(\mathrm{EHDA})_2\text{-}\mathrm{HPO_4}]}$$

At equilibrium, the solution containing $(\mathrm{EHDA})_2\text{-}\mathrm{HPO_4}$ would have more of the undissociated form than does the other solution, because more energy is required to break the chemical bonds of $(\mathrm{EHDA})_2\text{-}\mathrm{HPO_4}$ to form EHDA^+ and $\mathrm{HPO_4}^{-2}$. Thus the solution containing $\mathrm{EHDA_2\text{-}HPO_4}$ would exert a higher surface concentration according to the Langmuir adsorption isotherm if the equilibrium constant K_2 is less than K_1 since

$$K_2 = \frac{4[C_0 - [\mathrm{EHDA_2\text{-}HPO_4}]]^3}{[\mathrm{EHDA_2\text{-}HPO_4}]}$$

and

$$K_1 = \frac{[C_0 - [\mathrm{EHDA\text{-}H_2PO_4}]]^2}{[\mathrm{EHDA\text{-}H_2PO_4}]}$$

For the adsorption of ions, $\mathrm{HPO_4}^{-2}$ is strongly attracted by the layer of EHDA^+ on the surface, and is therefore better removed than the monovalent phosphate $(\mathrm{H_2PO_4}^-)$.

The higher value of $\mathrm{EHDA_2\text{-}HPO_4}$ in the bulk solution and the stronger attraction of $\mathrm{HPO_4}^{-2}$ would result in a higher surface concentration of phosphate when it is in the divalent form. This can be seen by the value of the ratio β_2/β_1. The preferential adsorption of phosphate could also be obtained through

$$\left(\frac{\Gamma_{\mathrm{HPO_4}^{-2}} + \Gamma_{\mathrm{EHDA_2-HPO_4}}}{\Gamma_{\mathrm{H_2PO_4}^-} + \Gamma_{\mathrm{EHDA-H_2PO_4}}}\right) = \frac{2\Gamma_{\mathrm{Br}^-} x_{\mathrm{HPO_4}^{-2}} (x_{\mathrm{Br}^-} 2x_{(\mathrm{EHDA})_2\mathrm{HPO_4}})/K_2 - (d\gamma/dx_{\mathrm{EHDA_2-HPO_4}})_{\mathrm{EHDA-Br}} x_{\mathrm{EHDA_2-HPO_4}}/RT}{\Gamma_{\mathrm{Br}^-} x_{\mathrm{H_2PO_4}^-}/K_1 - (d\gamma/dx_{\mathrm{EHDA-H_2PO_4}})_{\mathrm{EHDA-Br}} x_{\mathrm{EHDA-H_2PO_4}}/RT} \quad (16)$$

Even if K_1 and K_2 were known, the equation is difficult to apply since it requires careful measurements of all the species in the solution and the slope of the surface tension curves. The statistical analysis gives the ratio of Eq. (16) without the knowledge of K_1 and K_2 since

$$\frac{\beta_2}{\beta_1} = \frac{\Gamma_{HPO_4^{-2}} + \Gamma_{EHDA_2-HPO_4}}{\Gamma_{H_2PO_4^-} + \Gamma_{EHDA-H_2PO_4}}$$

when $X_1 = X_2$.

CONCLUSIONS

From the analysis of the experimental data, the following conclusions can be drawn.

(1) To attain the phosphate equilibrium surface concentration, a residence time of at least 7 sec should be allowed for the gas bubbles. The equilibrium residence time might be higher at low phosphate bulk concentrations due to the effect of the slow rate of arrival of molecules of surfactant-phosphate complex at the surface of the gas generating bubbles. To ensure surface saturation and to eliminate any possible experimental errors, a residence time of well over 7 sec (which is the value for a phosphate bulk concentration of approximately 3 ppm) is recommended.

(2) Comparison between $(\Gamma/\Gamma_e)_B$ and $(\Gamma/\Gamma_e)_{expt}$ at different residence times leads to the conclusion that the removal of phosphate is due to the adsorption of the ionic and conplex forms of phosphate with the surface potential set up by the presence of $EHDA^+$.

(3) The effect of pH and the bulk concentration on the equilibrium surface concentration was well described by a linear regression model (Eq. 23). The average absolute error is 16%. The surface concentration of phosphate attains its highest value when phosphate is in its divalent form because of the preferential adsorption of $H_2PO_4^{-2}$ and because of the presence of a large amount of the undissociated surfactant phosphate complex.

The removal of phosphate is approximately six times more efficient when phosphate is present in the divalent rather than the monovalent form.

(4) The rate of removal of phosphate can be described by a simple mass transfer equation:

$$d\Gamma/dt = h(\Gamma_e - \Gamma) \tag{5}$$

in which case h is determined from experimental data or by

$$\frac{d\Gamma}{dt} = B_2 \exp\left\{\frac{ze\psi_0 - W}{kt}\right\}(\Gamma_e - \Gamma) \tag{4}$$

in which case h is predicted from theory.

Good agreement has been found between the two different methods, especially in the range of pH where phosphate is in the monovalent form since Eq. (4) was calculated by the above assumption.

SYMBOLS

A	area available for ion on the surface, Å^2
D	dielectric constant of water
B_1, B_2	hydrodynamics constant, sec^{-1}
e	electronic charge, C
G	gas flow rate, cm^3/min
h	surface mass transfer coefficient, sec^{-1}
l	length of liquid pool, cm
K	Langmuir adsorption coefficient
K_1	equilibrium constant for $EHDAH_2PO_4$
K_2	equilibrium constant for $EHDA_2HPO_4$
k	Boltzmann constant
k'	constant ($k' = k \times 10^{16}$)
m	effective number of —CH_2— group in the hydrocarbon chain
N_{av}	Avogadro number
R	gas constant
T	absolute temperature, °K
t	residence time, sec
U_B	bubble velocity, cm sec^{-1}
x	concentration of phosphate or its complex, ppm of PO_4
X	total concentration of phosphate and its complex, ppm of PO_4
X_b	bulk phosphate concentration, ppm of PO_4
W	energy of desorption, cal
z	valency of surfactant ion
α	coefficient used in non linear model, sec^{-1}
β	coefficient used in linear model, g mole cm^{-2} ppm^{-1}
γ	surface tension, dyne cm^{-1}
Γ	surface concentration of phosphate, g mole cm^{-2}

θ	fraction of surface covered with molecule, ($\theta = \Gamma/\Gamma_0$)
μ	chemical potential, ergs
ρ	net charge density, C cm^{-3}
ψ_0	surface potential, mV

Subscripts

b	effluent or bulk concentration of phosphate
B	theoretical value of Γ/Γ_e
e	equilibrium or saturated concentration
expt	experimental value

Acknowledgments

Financial support was provided by the Department of Energy, Mines and Resources, Ottawa. Y. V. Nguyen was in receipt of a University of Toronto fellowship.

REFERENCES

1. D. L. Banfield and I. H. Newson, *Amer. Inst. Chem. Eng.-Ind. Chem. Eng., Symposium Series*, *1*, 3 (1965).
2. P. F. Wace and D. L. Banfield, *Chem. Process Eng.*, *47*, 70 (October 1966).
3. R. Grieves and D. Bhattacharyya, *Amer. Inst. Chem. Eng. J.*, *11*, 274 (1965).
4. R. Grieves and D. Bhattacharyya, *J. Appl. Chem.*, *18*, 149 (1968).
5. R. Grieves, D. Bhattacharyya, and C. J. Crandall, *J. Appl. Chem.*, *17*, 163 (1967).
6. L. Skrylev and S. Mokrushin, *Zh. Prikl. Khim.*, *37*, 211 (1964).
7. H. Shoen, E. Rubin, and D. Ghosh, *J. Water Pollution Control Fed.*, *34*, 10205 (1962).
8. D. McLean, J. Brown, and R. Laak, *J. Amer. Water Works Assoc.*, *58*, 7 (1966).
9. E. Hendrickson and C. Harding, *J. Air Pollution Control Assoc.*, *14*, 491 (1964).
10. R. Grieves and D. Bhattacharyya, *Separ. Sci.*, *1*, 81 (1966).
11. R. Grieves, *Brit. Chem. Eng.*, *13*, 1 (1968).
12. R. Grieves, *Separ. Sci.*, *1*, 4 (1966).
13. S. Primiani, "Continuous Foam Fractionation of Phosphate Using a Cationic Surfactant," M.A.Sc. Thesis, University of Toronto, December 1971.
14. J. T. Davies and E. K. Rideal, *Interfacial Phenomena*, Academic, N.Y., 1963.
15. A. W. Adamson, *Physical Chemistry of Surfaces*, Interscience, New York, 1960.
16. J. W. Gibbs, *Collected Works*, Vol. 1, Yale Univ. Press, New Haven, Connecticut, 1948, p. 219.
17. D. J. Nicklin, *Chem. Eng. Sci.*, *17*, 693 (1962).

Received by editor May 27, 1972